ELSEVIER

International Biodeterioration & Biodegradation, Vol. 39, No. 2–3 (1997) 235–243

PII: S0964-8305(97)00020-6
0964–8305 97 $17.00 – 0.00

Nondestructive Elemental Analysis of Wood Biodeterioration Using Electron Paramagnetic Resonance and Synchrotrons X-ray Fluorescence

B. L. Illman [a] & S. Bajt [b]

[a]*USDA/FS Forest Products Laboratory, Madison, WI 53705, USA*
[b]*University of Chicago, Chicago, IL 60637, USA*[1]

(Received 15 November 1996; accepted 10 January 1997)

Over the last few years we have developed nondestructive methods for the elemental analysis of wood during biodeterioration by fungi. In this paper we review progress made in our laboratories on the multi-element analysis of wood using electron paramagnetic resonance spectroscopy and synchrotron-generated X-ray spectroscopy. The non-intrusive sample preparation and the nondestructive methods have been used to detect elements *in situ* at concentrations as low as 0.1–10 ppm and to determine the redox states of several transition state metals. Custom specimen handling equipment and computer software were coupled with the analytical tools for mapping element accumulation and distribution. © 1997 Published by Elsevier Science Limited

INTRODUCTION

Elemental analysis of wood biodeterioration provides needed information about the chemical mechanisms of deterioration and the element requirements of deteriorating organisms. For several years, we have been developing systems for wood analysis by non-intrusive methods to detect the distribution and redox states of elements *in situ.* Most of our work has focused on biodeterioration of wood by basidiomycetous fungi. Many of the techniques are new to the area of wood chemistry. Our studies have concentrated on detecting redox states, distribution, mobilization, accumulation and neighboring atoms of specific elements, including manganese, iron, calcium, chromium, arsenic, zinc and copper. Wood deteriorating fungi require cations for key metabolic pathways and for mechanisms of wood deterioration (Evoki *et al.,* 1989; Highley *et al.,* 1994; Illman & Highley, 1989d; Jellison *et al.,* 1997). The detection of cation redox states and redox changes during deterioration provides needed information for determining and following chemical mechanisms of decay. Cation requirements and cation toxicity have been used to prevent fungal biodeterioration of wood, especially in the use of metal-based preservatives. The in-situ detection of redox states of metals in wood treated with metal-based preservatives answers questions about the toxic valence states of such metals as chromium and about the mechanisms of metal binding to wood.

Elemental analysis of specimens traditionally requires destructive techniques. Chemical methods to identify elements use mechanical grinding and chemical isolation or ashing procedures that are followed by separation techniques (HPLC, GC), resulting in mechanical and chemical destruction of specimens. Analysis by X-ray diffraction with scanning electron microscope (SEM) or transmission electron microscope (TEM) requires chemical treatment and destructive handling of specimens. Destructive elemental analysis raises questions about the production of artifacts in the data, about the in-situ nature and redox state of extracted elements and about their relatedness to neighboring elements. Analyzing wood for the elements involved in fungal biodegradation presents an additional problem because of the close proximity of wood structures and the offending organisms. usually fungi or bacteria.

We report here the progress made in our research on multi-element analysis of fungal wood biodeterioration *in situ* using electron para-

[1]Currently at Lawrence Livermore National Laboratory, Livermore. CA 94550.

magnetic resonance (EPR) and synchrotrons X-ray absorption techniques. The review is presented as an introduction to analytical tools that could be useful in other areas of biodeterioration and biodegradation.

ELECTRON PARAMAGNETIC RESONANCE

The usefulness of EPR (formerly designated ESR) arises from the fact that EPR can detect specific elements in a solid specimen (Knowles *et al.*, 1976). EPR is based on the interaction of electromagnetic radiation with the magnetic moments of unpaired electrons in a test specimen, i.e. with an electron that is unpaired with an oppositely directed spin of another electron. Elements with unpaired electrons have very specific EPR spectra. These include transition-metal ions such as Cr, Mn, Fe, Co, Cu and Mo. The unpaired electron spin system is also found in free radical molecules, such as oxygen free radical spin traps, low molecular weight spin label molecules used for lipids and some macromolecules exposed to X-irradiation.

The EPR spectrometer consists of a microwave klystron radiation source, a sample absorption cell in a microwave cavity sandwiched by magnets and a diode detector system sensitive to microwave frequencies. In the EPR spectrometer, the magnetic field is scanned instead of the microwave frequency and a reflection cavity system is used instead of a transmission system. The magnets in commercial EPR spectrometers produce magnetic fields in the region of 3 kG for 9 GHz (X-band) and 13 kG for 35 GHz (Q-band) spectrometers (Weil *et al.*, 1994). Magnetic field modulation enables signal amplification and use of phase-sensitive detection.

The sample is placed in a microwave cavity that is tuned to the klystron frequency to give maximum absorption. The magnetic field is modulated at the sample with a 100 kHz reference signal, producing an AC signal that is detected by a phase-sensitive detector (PSD). The PSD system filters out all signals other than the 100 kHz and produces a DC output signal to the oscilloscope pen recorder. The EPR spectrum, recorded as the magnetic field, is swept at a designated center of field and sweepwidth. Gauss are the commonly used units for expressing the magnetic field and spectral line splittings. The *g*- value is the absolute magnetic field position of the lines of an EPR spectrum and is typical for paramagnetic species. The g-value is calculated from the ratio of the klystron microwave frequency used in a given experiment to the magnetic field at which the center of spectrum occurs times 0.71444, Planck's constant/Bohr magneton (derived from the *g*-equation in Weil *et al.*, 1994).

When scanning a sample, the magnetic field position is scanned in the range of the published *g*-value for the metal or radical in question. Several experiment-dependent factors may cause the observed to vary from the published *g*- factor, especially the klystron microwave frequency (Weil *et al.*, 1994). By calculating *g* for each experiment, information can be obtained about the measured element or radical. Free radicals have resonances in the $g = 2$ region. Transition metals have g-values around 2.0-2.4 or from 1.4 to 9.7 (Weil *et al.*, 1994). The g-value can be helpful in identifying some magnetic species, but the value is not always specific for any one species. The minimum sample concentration is about 0.3 mM for metalloproteins, 5 mM for copper complexes, 0.1-1.0 µM for spin label with free radical intermediate and 0.3-0.5 mM spin label with lipid. Because EPR detects only elements with unpaired electrons in a specimen, the technique can be used to observe the effects of various treatments on the paramagnetism of the element, and thereby give information about the center of biochemical activity in the specimen. The generation of oxygen free radicals and the oxidation or reduction of transition state metals can be detected in the specimen.

EPR is a powerful tool to test a prominent hypothesis about transition metals and oxygen free radicals in the mechanism of brown-rot depolymerization of cellulose. The hypothesis states that depolymerization of cellulose involves Fenton chemistry in which Fe^{2+} reacts with hydrogen peroxide produced by the fungus (Illman & Highley, 1989a) to produce the hydroxyl radical (Cowling & Brown, 1969; Koenigs, 1974, 1975; Illman & Highley, 1989b; Chandhobe *et al.*, 1992). We predict that this highly reactive oxygen free radical would react with most chemicals, and that the radical would be produced near the carbohydrate in wood (Highley and Illman, 1991; Illman, 1992; Highley and Flournoy, 1994).

To study the role of cations in deterioration. we used EPR to analyze wood for the presence of manganese and iron cations in their various oxidation states (Illman *et al.*, 1988a,b, 1989b). Additionally, we used a spin-label probe method (Illman *et al.*, 1989b) to search for hydroxyl radical production during degradation and during growth

of fungi in chemically-defined culture medium. Iron oxidation states were not detected in wood at room temperature, prompting the use of more specific techniques (see synchrotrons sections below). A stable, hydroxyl radical-specific spin trap was used to scavenge and bind the radical as produced (Fig. 1). The hydroxyl radical was detected in wood and in fungal cultures (Illman *et al.*, 1988c,d; Highley & Illman, 1991).

The EPR spectrum for Mn^{2+} is given in Fig. 2, where aqueous $MnCl_2$ was used as the sample. The Mn^{2+} spectra has a sharp six-line configuration with the center of the field at 3330 Gauss and *g*-value at 2.0. The lines of the configuration can be slightly perturbed when ligands interact with divalent manganese. Aqueous Mn^{2+} can be detected at room temperature down to 5-10 µM, providing a simple means of identifying the cation and most interacting ligands.

The EPR spectra for Mn^{2+} for four species of wood are given in Fig. 3. The typical six-line configuration appears in cottonwood and white fir. The EPR spectra in the Mn^{2+} range in Douglas fir and redwood were not legible, indicating that divalent manganese was not present in wood or that substantial ligand interaction with Mn^{2+} occurred in these species (Illman *et al.*, 1988a,b, 1989a). The unknown Mn ligand would most likely be a low molecular weight wood component

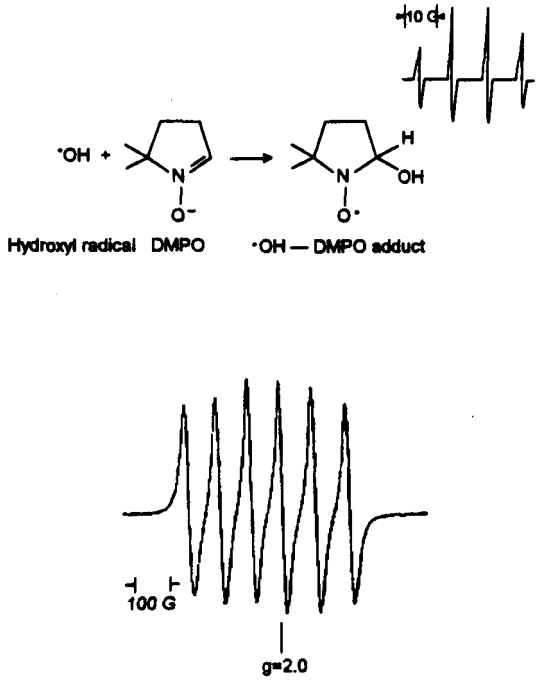

Fig. 2. Electron paramagnetic resonance spectrum of Mn^{2+} from aqueous $MnCl_2$ standard at 9.4 GHz. 25°C.

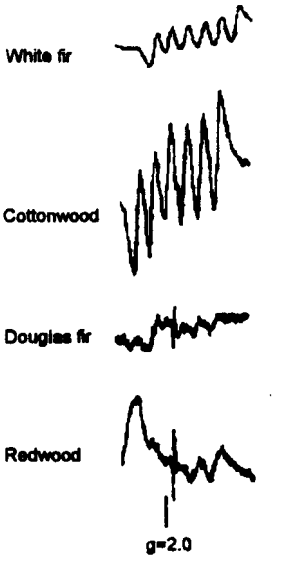

Fig. 3. Electron paramagnetic resonance spectra of Mn^{2+} in four species of wood.

(Illman, 1992). The spectra at $g = 2.0$ were consistently found in all experiments and could be used to fingerprint several of the wood species (Illman *et al.*, 1988a,b; Illman & Highley, 1989d).

The EPR signal for Mn^{2+} increased ten-fold in Douglas fir after two weeks of deterioration by the brown-rot fungus, *Gloeophyllum trabeum* (Fig. 4). The typical Mn^{2+} spectra appeared in Douglas fir after inoculation with *G. trabeum* and increased almost ten-fold after two weeks, an indication that the fungus altered and accumulated manganese during the deterioration process. The accumulated Mn^{2+} originated from within the wood after being released from the typical ligand binding or from reduction of Mn^{3+} or Mn^{4+} compounds in this wood species (Illman *et al.*, 1988b; Illman & Highley, 1989b). The redox state of the cation in Douglas fir and redwood could not be determined

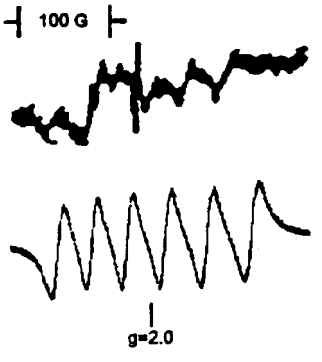

Fig. 4. Electron paramagnetic resonance spectra of Mn^{2+} in Douglas fir wood degraded by the brown-rot fungus *Gleophyllum trabeum.* Top = Douglas fir. bottom = Douglas fir + *G. trabeum.*

in these studies because EPR does not detect other redox states of manganese under the experimental conditions. The binding of manganese to wood and the role of this cation in fungal deterioration are discussed below in the synchrotrons sections.

A clearly resolved Mn^{2+} spectrum was detected in a control specimen of Southern yellow pine (shown in Fig. 3), increasing ten-fold over that of controls. The Mn^{2+} spectrum overlapped the hydroxyl radical spectrum found during the process of degradation by the brown-rot fungi, *Postia placenta* and *G. trabeum* (Illman ***et al.,*** 1989a,c). Manganese is known to replace iron in some reactions, raising questions about the possible role of the manganese redox states in the oxidative reactions of the deterioration process (Illman *et al.*, 1989b; Highley & Illman, 1991; Illman, 1992).

SYNCHROTRONS

Synchrotrons are powerful scientific instruments that produce electromagnetic radiation, including high energy X-rays and ultraviolet rays. Synchrotrons radiation can be used for a wide variety of X-ray-based techniques, including the detection of most elements of the periodic table. Synchrotrons are particle accelerators that consist of a source of electrons, a linear accelerator and a storage ring. Synchrotrons tend to be large instruments requiring supporting facilities, so scientists must travel to the facility to conduct experiments or send specimens for analysis by synchrotrons personnel. We have used the X-ray capabilities of the National Synchrotrons Light Source (NSLS) at Brookhaven National Laboratory for the nondestructive analysis of wood.

The production and use of synchrotrons radiation has been described in several publications (Winick & Doniack, 1980; Margaritondo, 1988; Jones, 1992). In synchrotrons, photons are emitted by charged particles (usually electrons) that are accelerated within the storage ring. When the electrons are of relativistic velocities. the emitted photons are in the X-ray region. The lifetime of the stored electrons can be as long as 24 h, making it a stable and reliable X-ray source. A portion of the X-radiation is allowed to escape from the storage ring by a beamline into specifically designed experimental stations.

Synchrotrons radiation has a wide and continuous spectrum and photons are highly polarized in the plane of the electron beam. The intensity of generated photons is many orders of magnitude higher than that from a conventional laboratory X-ray source. In addition, synchrotrons produced X-rays are naturally parallel in a vertical direction, an important feature for the development of a microbeam that can be used as a probe for low concentrations of elements (Gordon *et al.*, 1990a). A 5 μm microprobe can be readily constructed, properly aligned for good signal to noise ratio and used to detect trace elements in solid materials. A microprobe beamline has been constructed at NSLS on beamline X26A. A schematic view of the X-ray microprobe beamline at X26A is given in Fig. 5. An extensive tutorial review describing synchrotrons X-ray sources and beamlines is given by Smith (1995), with particular emphasis on applications for beamline X26A, the only hard X-ray microprobe operating today.

SYNCHROTRONS X-RAY FLUORESCENCE MICROPROBE

Synchrotrons X-ray fluorescence spectroscopy (SXRF) on the X26A microprobe can detect trace elements at a spatial resolution of 5 μm with high element sensitivity due to low background scattering (Hanson *et al.*, 1987; Gordon *et al.*. 1990b).

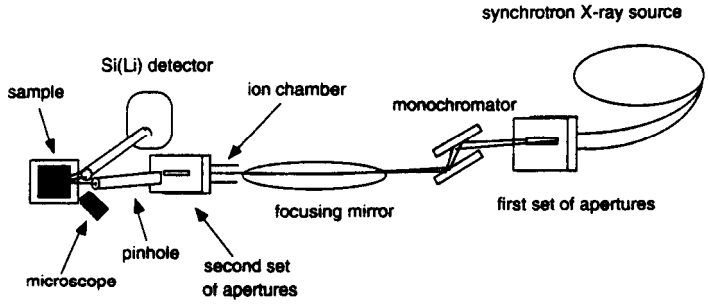

Fig. 5. Schematic of the X26A beamline at the National Synchrotrons Light Source

Elemental analysis using emission of characteristic X-rays is an established method. The process is briefly described in the following. When an incident photon ejects an electron from the atom in question, an electron hole is created, and the atom is ionized. When the electron hole is created, the excited atomic state decays either by an Auger process or by fluorescence. In the fluorescence process, the resulting vacancy is tilled by an outer shell electron, and a characteristic X-ray is emitted whose energy is unique for each transition that is used to identify the emitting atom. Transition filling vacancies in the innermost shell are called K X-rays, those tilling the next shell are L X-rays, etc. The intensity of a given fluorescent X-ray is proportional to the concentration of that element in the sample. Quantification of the element content based on XRF spectrum is relatively straight forward because the physics of photon interactions with matter is well understood.

The NSLS X26A beamline is used either in white beam mode or in monochromatic mode. White beam mode is utilized for quantitative X-ray fluorescence microanalysis. The white beam setup is much simpler than operating in the monochromatic mode. Two sets of apertures, a pinhole and a table with adjustable height on the top of which area sample stage, a detector and a microscope are sufficient to obtain a small beam spot with good signal to noise ratio.

The X-ray microprobe is situated on a bending magnet with an energy spectrum extending beyond 30 keV suitable for K-shell excitation to Z= 50 (Sn). Therefore, most elements above Na can be detected either by their K or L fluorescence lines. Detection limits with a 10 μm white beam vary between 0.1 and 10 ppm, depending on the element and the matrix being analyzed.

The microprobe has been used for many applications in the white beam mode, including the in-vivo elemental analysis of wood at a spot size of 5 μm (Fig. 6), the study of the effectiveness of different treatment strategies on acid papers using trace element distributions (Zappala *et al.*, 1996), and element distribution across annual tree rings to determine the cause of stain in prime timber (Illman, unpublished). The distribution of manganese in spruce tree rings demonstrated that high concentrations of the cation, as indicated by peaks in the spectrum, correspond to dark stains in the wood. After locating the distribution and ratio of elements *in situ* by XRF, the oxidation state of key elements can be detected and mapped in deteriorating or stained wood.

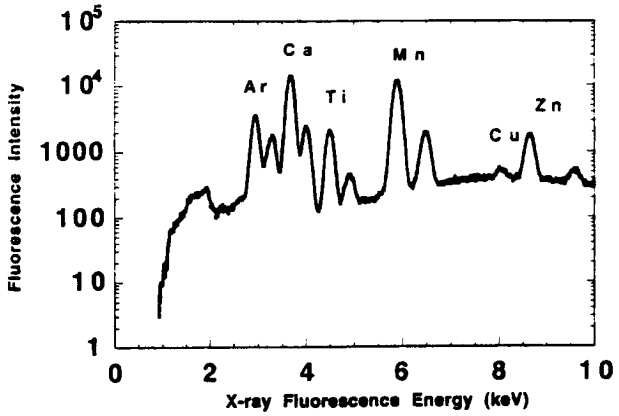

Fig. 6. Synchrotrons X-ray fluorescence of a 5 μm spot on Southern yellow pine wood.

X-RAY ABSORPTION SPECTROSCOPY

Information on the chemical state of elements (redox state and coordination geometry) can be extracted from an X-ray absorption spectrum. The spectrum can be subdivided into two energy regions. The region around the sharp absorption edge is called the X-ray Absorption Near Edge Structure (XANES) and the region at energies above the absorption edge (about 1000 eV wide) is the Extended X-ray Absorption Fine Structure (EXAFS). The XANES and EXAFS spectroscopies refer to the measurement of the X-ray absorption coefficient as a function of photon energy. When the X-ray energy is tuned to the binding energy of some core level of an atom, an abrupt increase in the absorption coefficient occurs, giving an absorption edge. Near and below the absorption edge there may also be absorption peaks that are due to excitations of core electrons to some bound states. The effects around and on the absorption edge are difficult to describe theoretically because they are due to many-body interactions and multiple scattering. Modulations of the absorption coefficient above the absorption edge (EXAFS) on the other hand are understood as interference effects involving scattering of the outgoing photoelectron from the neighboring atoms (Teo, 1986) and can be calculated using computer codes such as FEFF (Zabinsky *et al.*, 1995; Rehr *et al.*, 1991). A monochromatic beam is needed to measure these spectra. Standard EXAFS and XANES measurements are made by using relatively large X-ray beams and thick specimens. Absorption measurements have very low signal to noise ratios at elemental concentrations at less than 1% Therefore, diluted samples require fluorescent

X-ray detection, which can be accomplished with either a single- or 13-element energy dispersive detector (Cramer *et al.,* 1988).

A schematic of the X26A beamline in monochromatic mode is given in Fig. 5. A monochromator, a channel-cut silicon (111) crystal, is used to select a desired X-ray energy interval. Since only a very narrow band of the whole spectrum is selected, the intensity of the monochromatic beam is much lower as compared to the white beam. To guide X-rays to the sample without any further major loss of intensity, an X-ray mirror is placed in the beamline to focus the spot on the sample. Before reaching the sample, X-rays have to pass through a second set of slits to stop any scattered X-rays. A third set of slits, also called a pinhole, is placed in front of the sample to cut X-rays down to a 1–5 μm beam spot. The beamline is under high vacuum until it enters a lead-lined room (hutch). Experimental stations inside the hutch contain the sample, the detector, the microscope and video equipment and are maintained in ambient condition at room temperature. Therefore, it is very easy to handle various sample sizes, change the samples, or change the experimental setup. A series of safety interlocks prevents X-rays from entering the beamline or the hutch until the doors of the hutch are locked for the experiment.

Only a small amount of the sample is needed for the measurement and no special sample preparation is necessary. The measurements are taken *in situ* without destruction of the sample. The sample is mounted on a computer controlled sample stage and can be rotated or moved relative to the X-ray beam in *x*-, *y*- and *z*- directions. The position of the specimen is viewed throughout the experiment on a video screen connected to a CCD camera mounted on a microscope inside the hutch. The X-ray beam hits the specimen at a 45° angle (Fig. 5). An energy dispersive detector is placed at 90° towards the incoming beam. This angle provides the best peak to background ratio.

X-ray absorption spectra are collected when a beamline is operating in monochromatic mode. X-ray absorption near edge structure (XANES) provides information on the local environments (within a few A) of the atom of interest in different materials. The XANES spectra are obtained by scanning the monochromator in small energy steps across the absorption edge and measuring the fluorescence intensity of the element of interest as a function of the incident energy. The valence of the element is reflected in absorption edge position. The valence changes from one redox state of the element to another are observed as an eV shift of the absorption edge. An example of manganese XANES spectra is given in Fig. 7, showing the eV change between Mn^{2+} and Mn^{3+}. We have used XANES to detect Mn^{2+}, Mn^{3+} and Mn^{4+} in wood during decay by brown- and white-rot fungi (Illman *et al.,* 1994). The method will allow us to answer questions that were raised by EPR data. What is the oxidation state of Mn in wood? Where is Mn found in wood? By preparing images of oxidation state distribution we expect to locate Mn oxidizing or reducing agents in relation to wood and fungal structures. The method will be used to evaluate the role of this cation in the process of deterioration and pin-point the location of redox state changes in wood at early and late stages of decay.

In addition to the absorption edge shifts, some pre-edge peaks are often used to quantify the ratio of different oxidation states. In the case of chromium for example, the pre-edge peak intensity change is used to quantify the amount of toxic Cr^{6+} in the specimen. This technique was originally developed to-determine the chromate content in low-level radioactive waste (Bajt *et al.,* 1993). The technique was used to study metal redox states in wood treated with the preservative chromated copper arsenate (CCA). XANES spectra were obtained for chromium in CCA-treated wood two years after treatment (Illman *et al.,* 1994a) and in CCA-treated wood that had been degraded by a unique isolate of a brown-rot fungus (Illman *et al.,* 1996). XANES spectra for Cr^{3+} and Cr^{6+} standards are given in Fig. 8. The less toxic, more stable Cr^{3+} was detected in CCA-treated controls

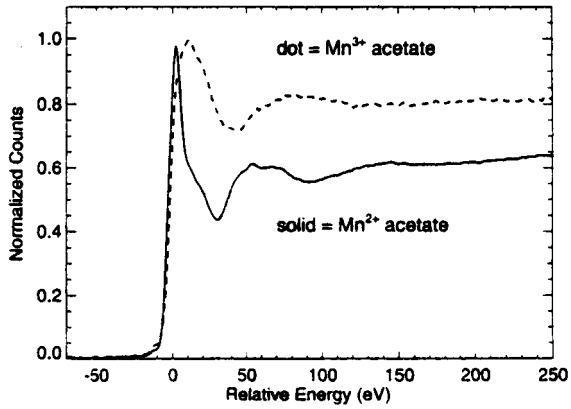

Fig. 7. Synchrotron-generated XANES spectra of Mn^{2+} and Mn^{3+} standards.

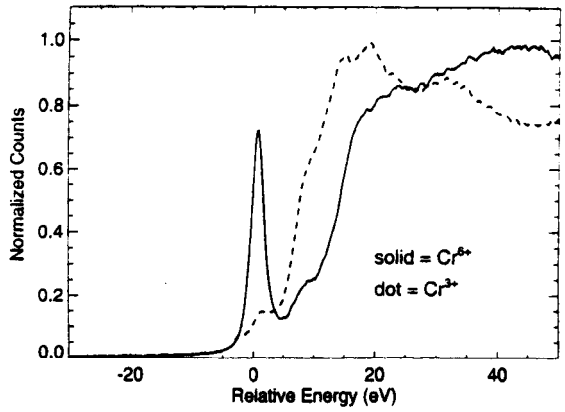

Fig. 8. Synchrotron-generated XANES spectra of Cr^{6+} and Cr^{3+} standards.

and in fungal degraded wood, indicating that the fungus had not reduced the cation to the more toxic Cr^{6+} form. We are currently analyzing the same specimen for copper and arsenic redox states.

Pre-edge peak position shifts are in many cases more reliable for quantitative determination of oxidation state than the absorption edge shifts. For example, a linear relationship between the pre-edge peak positions of fayalite, Fe_2SiO_4(pure Fe^{2+}), magnetite, Fe_3O_4(0.66% Fe^{3+}) and hematite, Fe_2O_3(pure Fe^{3+}) and their known oxidation state was observed and used to quantify the Fe^{2+}/Fe^{3+} ratio in different iron bearing materials (Bajt *et al.*, 1994; Delaney *et al.*, 1996). Relative pre-edge peak positions in Fe XANES spectra of fayalite, magnetite and hematite standards are shown in Fig. 9. By using pre-edge peak positions of Fe standards, the Fe XANES spectra in Southern yellow pine were obtained during decay by brown-rot fungi. The fungi accumulated Fe into the decayed wood, producing an Fe^{2+}/Fe^{3+} ratio that was higher than controls (Illman *et al.*, 1995),

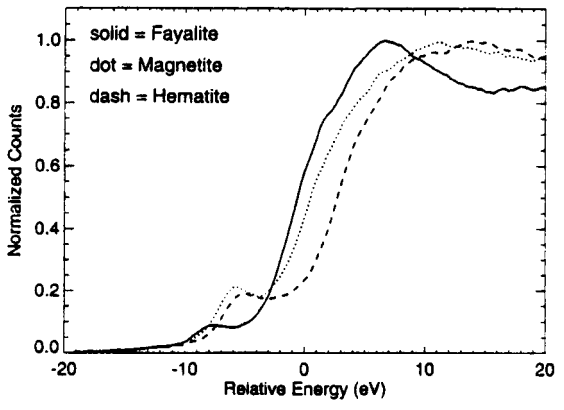

Fig. 9. Synchrotron-generated XANES spectra of Fe^{2+} and Fe^{3+} standards.

lending support to the hypothesis that Fe is involved in fungal deterioration (Goodell *et al.*, 1995; Hiramo *et al.*, 1995; Green & Highley, 1997).

SUMMARY

The use of nondestructive methods for the in-situ elemental analysis of specimens has provided a unique opportunity to 'view' the function of deteriorating fungi and the chemical components of their wood food source. In the near future, we expect elemental analysis to be available for 3-dimensional images of solid specimens through the use of computer assisted tomography (Illman & Dowd, 1996, 1997). The EPR, XRF and XANES techniques described in this review are applicable to all areas of biodeterioration and biodegradation, especially where metal oxidation—reduction reactions are suspected.

REFERENCES

Bajt, S., Clark, S. B., Sutton, S. R., Rivers, M. L. & Smith & . J. V. (1993) Synchrotron X-ray determination of chromate content using X-ray absorption near-edge structure. *Analytical Chemistry*, **65**, 1800–1804.

Bajt, S., Sutton, S. R. & Delaney, J. S. (1994) X-ray microprobe analysis of iron oxidation states in silicates and oxides using X-ray absorption near edge structure (XANES). *Geochimica et Cosmochimica Acta*, **58**, 5209–5214.

Chandhoke, V., Goodell, B., Jellison, J. & Fekete, F. A. (1992) Oxidation of KTBA by iron-binding compounds produced by the wood-decaying fungus *Gloeophyllum trabeum*. *FEMS Microbiology Letters*, **90**, 236–266.

Cowling, E. B. & Brown, W. (1969) Structural features of cellulosic materials in relation to enzymatic hydrolysis. In *Cellulases and Their Applications, Advance Chemical Series*, eds G. J. Hajuy & E. T. Reese Vol. 95, pp. 152–187.

Cramer, S. P., Tench, O., Yocum, M. & George, G. N. (1988) A 13 element Ge-detector for fluorescence EXAFS. *Nuclear Instruments and Methods*, **A266**, 586–591.

Delaney, J. S., Bajt, S., Sutton, S. R. & Dyar, M. D. (1996) *In situ* microanalysis of Fe^{3+}–^{183}Fe in amphibole by X-ray absorption near edge structure (XANES) spectroscopy. In *Mineral Spectroscopy: A Tribute to Roger G. Burns*, eds M. D. Dyar, C. McCammon & M. W. Schaefer, No. 5, pp. 165–171. The Geochemical Society, Special Publication, Houston, TX.

Enoki, A., Tanaka, H. & Fuse, G. (1989) Relationship between degradation of wood and production of H_2O_2 producing one-electron oxidases in brown-rot fungi. *Wood Science and Technology*, **23**, 1–12.

Goodell, B., Liu, J., Jellison, J., Lu, J., Paszczynske, A. & Fekete, F. (1995) Chelation activity and hydroxyl radical production mediated by low molecular weight phenolate compounds isolated from *Gloeophyllum trabeum*. In *Biotechnology in the Pulp and Paper Industry*, eds E. Srebotnik & K. Messner, pp. 591–594. Facultas-Univeritatsvewriag, Vienna, Austria.

Gordon, B. M., Jones, K. W., Hanson, A. L., Pounds, J. G., Rivers, M. L., Spanne, P. & Sutton, S. R. (1990a) An X-ray microprobe facility using synchrotron radiation. In *Biological Trace Element Research*, ed. G. N. Schrauzer, pp. 133–141. The Humana Press Inc, Totowa, NJ.

Gordon, B. M., Hanson, A. L., Jones, K. W., Pounds, J. G., Rivers, M. L., Schidlovsky, G., Spanne, P. & Sutton, S. R. (1990b) The application of synchrotron radiation to microprobe trace-element analysis of biological samples. *Nuclear Instruments and Methods*, **B45**, 527–531.

Green, F. III & Highley, T. L. (1997) Mechanism of brown-rot decay: paradigm or paradox. *International Biodeterioration & Biodegradation*, **39**(2–3), 113–124.

Hanson, A. L., Jones, K. W., Gordon, B. M., Pounds, J. G., Kwiatek, W., Rivers, M. L., Schidlovsky, G. & Sutton, S. R. (1987). Trace element measurements using synchrotron radiation. *Nuclear Instruments and Methods*, B24 25, 400–404.

Highley, T. L. & Flournoy, D. S. (1994) Decomposition of cellulose by brown-rot fungi. In *Recent Advances in Biodeterioration and Biodegradation*, eds K. L. Garg, Neelima Garg & K. J. Mukerji, Vol. II, pp. 191–221. Plenum Press, NY.

Highley, T. L. & Illman, B. L. (1991) Progress in understanding how brown-rot fungi degrade cellulose. *Biodeterioration Abstracts*, **5**, 231–244.

Highley, T. L., Clausen, C. A., Croan, S. C., Green, F. III, Illman, B. L. & Micales, J. A. (1994) Research on Biodeterioration of Wood, 1987–1992. USDA/FS Forest Products Laboratory Research Paper, FPL-RP-529.

Hirano, T., Tanaka, H. & Enoki, A. (1995) Extracellular substance from the brown-rot fungus *Tyromyces palustris* that reduces molecular oxygen to hydroxyl radicals and ferric iron to ferrous iron. *Mokuzai Gak.*, **41**, 334–341.

Illman, B. L. (1992) Oxidative degradation of wood by brown-rot fungi. In *Active Oxygen/Oxidative Stress and Plant Metabolism, Current Topics in Plant Physiology*, eds E. J. Pell, K. L. Steffen & J. C. Shannon, Vol. 6, pp. 97–106. American Society of Plant Physiologists, Rockville, MD.

Illman, B. L. & Dowd, B. (1996) Microtomography of wood degraded by fungi. National Synchrotron Light Source Activity Report BNL. Brookhaven National Laboratory and Associated Universities. National Technical Information Service, Springfield, VA.

Illman, B. L. & Dowd, B. (1997) Synchrotron applications in forestry and forest products. *Synchrotron Radiation News*, **10**(2), 18–23.

Illman, B. L. & Highley, T. L. (1989a) Hydrogen peroxide formation by wood decay fungi in liquid medium. (Abstr.). *Phytopathology*, **78**, 617.

Illman, B. L. & Highley, T. L. (1989b) Decomposition of wood by brown-rot fungi. In *Biodeterioration Research II*, eds G. C. Llewellyn & C. E. O'Rear, pp. 465–484. Plenum Press, NY.

Illman, B. L., Meinholtz, D. C. & Highley, T. L. (1988a) Diagnosis of wood decay using ESR (Abstr.). International Research Group on Wood Preservation Series.

Illman, B. L., Meinholtz, D. C. & Highley, T. L. (1988b) An electron spin resonance study of manganese changes in wood decayed by the brown-rot fungus, *Postia placenta*. International Research Group on Wood Preservation Series, Document IRG/WP-1359.

Illman, B. L., Meinholtz, D. C. & Highley, T. L. (1988c) Generation of hydroxyl radical by the brown-rot fungus, *Postia placenta*. International Research Group on Wood Preservation Series, Document IRG/WP-1360.

Illman, B. L., Meinholtz, D. C. & Highley, T. L. (1989a) Manganese as a probe of fungal degradation of wood. In *Biodeterioration Research II*, eds G. C. Llewellyn & C. E. O'Rear, pp. 485–496. Plenum Press, NY.

Illman, B. L., Meinholtz, D. C. & Highley, T. L. (1989b) Oxygen free radical detection in wood colonized by the brown-rot fungus, *Postia placenta*. In *Biodeterioration Research II*, eds G. C. Llewellyn & C. E. O'Rear, pp. 497–509. Plenum Press, NY.

Illman, B. L., Bajt, S. & Sutton, S. R. (1994a) Micro-XANES analysis of chromium in wood treated with chromated-copper-arsenate (CCA). National Synchrotron Light Source, Activity Report: BNL-52455. Brookhaven National Laboratory and Associated Universities. National Technical Information Service, Springfield, VA.

Illman, B. L., Schulze, D. G., Bajt, S. & Sutton, S. R. (1994b) Manganese detection in wood using X-ray absorption near edge structure. National Synchrotron Light Source Activity Report BNL-52455. Brookhaven National Laboratory and Associated Universities. National Technical Information Service, Springfield, VA.

Illman, B. L., Bajt, S. & Patterson Nuessle (1995) Micro-XANES of iron redox states in wood during degradation by fungi. National Synchrotron Light Source Activity Report BNL. Brookhaven National Laboratory and Associated Universities. National Technical Information Service, Springfield, VA.

Illman, B. L., Bajt, S. & Highley, T. L. (1996) Fungal degradation of wood treated with metal-based preservatives: II. Redox states of chromium. International Research Group on Wood Preservation Series, Document IRG/WP 96-10164.

Jellison, J., Connelly, J., Goodell, B., Doyle, B., Illman, B., Fekete, F. & Ostrofsky, A. (1997) The role of cations in the biodegradation of wood by the brown-rot fungi. *International Biodeterioration & Biodegradation*, **39**(2–3), 165–179.

Jones, K. W. (1992) Synchrotron radiation-induced X-ray emission. In *Handbook of X-ray Spectrometry, Methods and Techniques*, eds R. E. Van Grieken & A. A. Markowicz, pp. 411–452. Marcel Dekker, New York.

Knowles, P. F., Marsh, D. & Rattle, H. W. E. (1976) *Magnetic Resonance of Biomolecules*. John Wiley, New York.

Koenigs, J. W. (1974) Hydrogen peroxide and iron: A proposed system for decomposition of wood by brown-rot basidiomycetes. *Wood and Fiber Science*, **6**, 66–80.

Margaritondo, G. (1988) *Introduction to Synchrotron Radiation*. Oxford University Press, New York.

Rehr, J. J., Mustre de Leon, J., Zabinsky, S. I. & Albers, R. C. (1991) Theoretical X-ray absorption fine structure standards. *Journal of the American Chemical Society*, **113**, 5135–5140.

Smith, J. V. (1995) Synchrotron X-ray source: Instrumental characteristics. New applications in microanalysis, tomography, absorption spectroscopy and diffraction. *Analyst*, **120**, 1231–1245.

Teo, B. K. (1986) *EXAFS: Basic Principles and Data Analysis*. Springer, Berlin.

Weil, J. A., Bolton, J. R. & Wertz, J. E. (1994) *Electron Paramagnetic Resonance: Elementary Theory and Practical Applications*. John Wiley, New York.

Winick, H. & Doniack, S. eds (1980) *Synchrotron Radiation Research*. Plenum Press, New York.

Zabinsky, S. I., Rehr, J. J., Ankudinov, A., Albers, R. C. & Eller, M. J. (1995) Multiple-scattering calculations of X-ray-absorption spectra. *Physical Review*, **B52**, 2995–3009.

Zappala, A., Bajt, S., Gigante, G. E. & Hanson, A. L. (1996) Applications of EDXRF in the conservation of acid papers using synchrotron light microbeam. *Nuclear Instruments and Methods*, **B 117**, 145–150l.